Multi-scale geometrical Lagrangian statistics: Extensions and applications to particle-laden turbulent flows

By B. Kadoch†, M. Bassenne, M. Esmaily-Moghadam, K. Schneider†, M. Farge¶ AND W. J. T. Bos‖

We present multi-scale statistics of particle trajectories in isotropic turbulence and compare the behavior of fluid and inertial particles. The directional change of inertial particles is quantified by considering the curvature angle for different time increments. Distinct scaling behaviors of the mean angle are observed for short, intermediate and long time lags. We also introduce the scale-dependent torsion angle, which quantifies the directional change of particles moving out of a reference plane. The influence of the Stokes number on the mean angles and on the probability distributions are analyzed. Finally, we assess the impact of LES and particle SGS modeling on these statistics.

1. Introduction

Modeling particle dispersion in turbulent flows is a major challenge for predictive science. In the context of Eulerian turbulence modeling, developing particle subgrid scale (SGS) models which yield reliable results is still an ongoing research area. However, significant progress during recent decades has been made in the Lagrangian characterization of turbulence, from both an experimental and a numerical viewpoint, see Yeung (2002); Toschi & Bodenschatz (2009). An important field of application, which motivates the present work, is that of particle-based solar receivers, which are more efficient than conventional ones in which a solid surface absorbs the solar radiation and transfers the heat to an operating fluid. Particle-based receivers use fine grains suspended in the fluid to transfer heat throughout the fluid volume, aiming to improve the heat-transfer efficiency (PSAAPII 2016, http://exascale.stanford.edu/). Another application of such systems is to generate very high local temperature through strong particle segregation and use it for endothermic chemical reactions. Accurate turbulence SGS models for particles are attractive tools to reduce the computational cost associated with their optimization through Large-Eddy Simulations (LES). A prerequisite for developing such models is the detailed understanding of the geometrical properties of particle dynamics.

Different tools for performing geometrical statistics of particles have been developed and a recent overview can be found, for instance, in Braun *et al.* (2006). For example, the curvature and torsion of fluid trajectories in isotropic turbulence have been analyzed in Scagliarini (2011). In Bos *et al.* (2015), we analysed the directional change of particles in isotropic turbulence using a new multi-scale measure, the scale-dependent curvature angle of trajectories. It quantifies the direction of motion over successive time intervals. This measure was originally introduced in Burov *et al.* (2013) for studying complex dynamics

† Aix-Marseille Université, France
¶ Ecole Normale Supérieure, France
‖ Ecole Centrale de Lyon, France

in the context of mesoscopic systems. For fluid particles in isotropic three-dimensional turbulence Bos *et al.* (2015) showed that the inertial range of turbulence is directly related to the angular statistics of Lagrangian fluid particle trajectories. A self-similar behavior of the probability density function of the directional change has also been identified. Kadoch *et al.* (2016) used this measure to carry out statistical analyses of fluid particle trajectories in two-dimensional turbulence, either in periodic domains, for both the direct and inverse energy cascade, or in confined circular domains. We found that the influence of flow confinement is reflected in the long-time behavior of the angular statistics. The expected long-term outcome of these analyses is the development of accurate models for the topology of Lagrangian trajectories in dispersion models.

The aim of the paper is to perform statistical analyses of scale-dependent angles of particle trajectories in isotropic turbulent flows. Besides fluid particles, that were investigated in Bos *et al.* (2015), we extend the geometrical statistics to inertial particles and study the influence of the Stokes number. In addition to the multi-scale curvature angle, we introduce a new statistical measure, the multi-scale torsion (or dihedral) angle. This angle quantifies the three-dimensionality of the particle trajectory at different scales. Mean values and probability distribution functions of both scale-dependent quantities are analyzed for DNS data. We also assess the impact of LES and particle SGS models on the above statistics.

The remainder of the paper is organized as follows. After summarizing the simulation data of particle-laden flows in Section 2, we describe the multi-scale geometric statistics in Section 3. The results are discussed in Section 4, and some conclusions and perspectives for future work are given in Section 5.

2. Simulation data of particle-laden flows

In the following we give a short description of the turbulence and particle database used in this study, as well as the Lagrangian description of the particle motion. Further details on the flow data can be found in Esmaily-Moghadam & Mani (2015). We consider DNS of isotropic turbulence at a Taylor micro-scale Reynolds number $Re_\lambda = 100$. We maintain turbulence using a linear forcing term on the right-hand side of the Navier–Stokes equation (Bassenne *et al.* 2016). We use second-order finite differences on a 256^3 staggered grid in all computations.

Five classes of particles are simulated at Stokes numbers $0, 1/16, 1, 4$ and 16. We compute the Stokes number as the ratio of particle relaxation time $\tau = \rho_p d_p/18\mu$, where ρ_p is the particle density, d_p is the particle diameter, and μ is the dynamic fluid viscosity, to the Kolmogorov time scale $\tau_k = \sqrt{\nu/\epsilon} = 2 \times 10^{-6}$. At $\mathrm{St} = 0$, the trajectory of a fluid particle $\boldsymbol{X}(t)$ advected by the velocity field $\boldsymbol{u}$ is described by the ordinary differential equation $d\boldsymbol{X}/dt = \boldsymbol{u}(\boldsymbol{X}(t), t)$. For inertial particles, the trajectory $\boldsymbol{X}_p(t)$ is modeled by $d\boldsymbol{X}_p/dt = \boldsymbol{u}_p$, where $\boldsymbol{u}_p$ is the particle velocity defined by $d\boldsymbol{u}_p/dt = (\boldsymbol{u}(\boldsymbol{X}_p) - \boldsymbol{u}_p)/\tau$. This one-way coupled point-particle model is employed in the computations. To initialize these simulations, we seed the computational domain by $100,000$ homogeneously distributed particles of each class. Then, the governing equations are integrated for $200\,\tau_k$ in a statistically stationary regime to ensure particle clustering is fully established. Apart from Re_λ, $\mathrm{St} = \tau/\tau_k$ is the only non-dimensional parameter that governs the behavior of this system. In physical terms, the Stokes number represents the tendency of particles to follow the flow. In the limit $\mathrm{St} \to 0$, the particles become fluid tracers, while at St

$\to \infty$, they are completely ballistic and follow trajectories that are independent of the background flow. In the next sections, we study the effect of St on Lagrangian statistics.

3. multi-scale geometric Lagrangian statistics

Geometric Lagrangian statistics are conveniently described using some tools from differential geometry. Frenet–Serret formulas, for example, see Braun *et al.* (2006), are used to define a local coordinate system of the trajectory, defined by the curve, $\boldsymbol{x}(t)$. The arclength is given by $ds = \sqrt{(d\boldsymbol{x}(t)/dt)^2}dt$ and correspondingly we can expand $\boldsymbol{x}(s)$ in a Taylor series in a neighborhood of a given point. The smoothness of the trajectories in turbulent flows which allows such an expansion has been shown in Constantin *et al.* (2015). Subsequently we obtain the tangent vector $\boldsymbol{t} = d\boldsymbol{x}(t)/ds$, the normal vector $\kappa\boldsymbol{n} = d^2\boldsymbol{x}(t)/ds^2$ and the binormal vector $\boldsymbol{b} = \boldsymbol{t} \times \boldsymbol{n}$. All three vectors are unit vectors which are orthogonal to each other. These three vectors form a coordinate system and allow us to introduce a system of nine ODEs, $d\boldsymbol{t}/ds = \kappa\boldsymbol{n}, d\boldsymbol{n}/ds = \vartheta\boldsymbol{b} - \kappa\boldsymbol{t}, d\boldsymbol{b}/ds = -\vartheta\boldsymbol{n}$ which describe a curve uniquely for given initial conditions, $\boldsymbol{t}(s=0), \boldsymbol{n}(s=0)$ and $\boldsymbol{b}(s=0)$. The two continuous functions $\kappa(s) \geq 0$ and $\vartheta(s)$ denote the curvature and the torsion, respectively. The torsion is defined by $\vartheta = 1/\kappa^2 \det\left(d\boldsymbol{x}(s)/ds, d^2\boldsymbol{x}(s)/ds^2, d^3\boldsymbol{x}(s)/ds^3\right)$ and we thus need $d^3\boldsymbol{x}(s)/ds^3$. Fixing the initial position of the curve, $\boldsymbol{x}(s=0) = \boldsymbol{x}_0$, we obtain $\boldsymbol{x}(s) = \boldsymbol{x}_0 + \int_0^s \boldsymbol{t}(s')\, ds'$.

3.1. *Curvature and scale-dependent curvature angle*

The curvature of the fluid-particle trajectory is defined by

$$\kappa(t) = \frac{|\boldsymbol{u} \times \boldsymbol{a}|}{|\boldsymbol{u}|^3} = \frac{a_\perp}{u^2}\,, \tag{3.1}$$

where u and $a_\perp$ are the magnitude of the velocity and of the normal or perpendicular acceleration, respectively. Note that $\kappa(t) \geq 0$. For $\kappa = 0$, the particle velocity and the acceleration vectors are parallel.

Introducing time increments of the Lagrangian particle position,

$$\delta\boldsymbol{X}(\boldsymbol{x}_0, t, \tau) = \boldsymbol{X}(\boldsymbol{x}_0, t) - \boldsymbol{X}(\boldsymbol{x}_0, t-\tau)\,,$$

where $\boldsymbol{X}(\boldsymbol{x}_0, t)$ is the position of a particle at time t, passing through point $\boldsymbol{x}_0$ at time $t = t_0$, we can define the curvature angle $\Theta(t, \tau)$ by

$$\cos(\Theta(t,\tau)) \;=\; \frac{\delta\boldsymbol{X}(\boldsymbol{x}_0, t, \tau) \cdot \delta\boldsymbol{X}(\boldsymbol{x}_0, t+\tau, \tau)}{|\delta\boldsymbol{X}(\boldsymbol{x}_0, t, \tau)|\,|\delta\boldsymbol{X}(\boldsymbol{x}_0, t+\tau, \tau)|}\,. \tag{3.2}$$

This quantity describes the directional change of a fluid-particle in the plane for a given scale, i.e., the increment size τ. An illustration of Θ is given in Figure 1, left.

The ensemble average of this curvature angle will be denoted by

$$\theta(\tau) \equiv \langle|\Theta(t,\tau)|\rangle\,. \tag{3.3}$$

At short times, we expect that $\theta(\tau)$ tends to zero, which means that particles have the tendency to go straight. At long times, the curvature angle should tend to the asymptotic value $\pi/2$, which corresponds to the mean angle assumed by three random points in an infinite domain and thus to their decorrelation.

The curvature κ is obtained in the limit when the increment size tends to zero, namely,

$$\kappa(t) = \lim_{\tau\to 0} \frac{|\Theta(t,\tau)|}{2\tau\|\boldsymbol{u}(t)\|}\,. \tag{3.4}$$

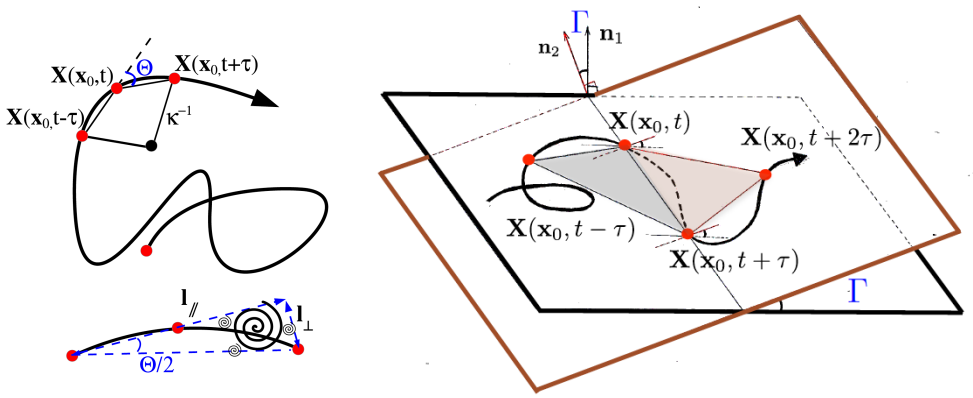

FIGURE 1. Left: illustration of the curvature angle (from (Bos *et al.* 2015)). Right: illustration of the torsion angle.

For inertial particles, we can define the curvature angle analogously by replacing $\boldsymbol{X}$ by $\boldsymbol{X}_p$.

3.2. *Torsion and scale-dependent torsion angle*

The torsion of the fluid particle trajectory is defined by

$$\vartheta(t) = \frac{\boldsymbol{u}\cdot(\boldsymbol{a}\times\dot{\boldsymbol{a}})}{\kappa^2\, u^6} = \frac{\boldsymbol{u}\times\boldsymbol{a}}{\|\boldsymbol{u}\times\boldsymbol{a}\|^2}\cdot\dot{\boldsymbol{a}}\,, \tag{3.5}$$

where $\dot{\boldsymbol{a}}t$ is the time derivative of the acceleration. Note that $\vartheta(t)$ is a signed quantity, which is directly related to the kinetic helicity $h = \boldsymbol{\omega}\cdot\boldsymbol{u}$ of the flow (Sposito 2001) as

$$\vartheta = \frac{1}{2}\,\frac{\boldsymbol{\omega}\cdot\boldsymbol{u}}{u^2}\,.$$

If the torsion vanishes, $\vartheta = 0$, then the particle velocity, acceleration and its derivative are coplanar vectors.

The torsion angle, also called dihedral angle (the angle between two intersecting planes), can be defined as

$$\cos(\Gamma(t,\tau)) = \frac{[\delta\boldsymbol{X}(\boldsymbol{x}_0,t-\tau,\tau)\times\delta\boldsymbol{X}(\boldsymbol{x}_0,t,\tau)]\cdot[\delta\boldsymbol{X}(\boldsymbol{x}_0,t,\tau)\times\delta\boldsymbol{X}(\boldsymbol{x}_0,t+\tau,\tau)]}{|\delta\boldsymbol{X}(\boldsymbol{x}_0,t-\tau,\tau)\times\delta\boldsymbol{X}(\boldsymbol{x}_0,t,\tau)|\,|\delta\boldsymbol{X}(\boldsymbol{x}_0,t,\tau)\times\delta\boldsymbol{X}(\boldsymbol{x}_0,t+\tau,\tau)|} \tag{3.6}$$

for a given time increment τ. This quantity describes the directional change of a particle for a given scale, i.e., the increment size τ, but now in space. It thus measures the angle at which the particle leaves a reference plane. An illustration of Γ is given in Figure 1, right.

Similar to the curvature angle, we can define the ensemble average of the torsion angle, which will be denoted by

$$\gamma(\tau) \equiv \langle|\Gamma(t,\tau)|\rangle\,. \tag{3.7}$$

Again, we expect for small time lags τ that γ tends to zero, and that the particles stay in the plane. Because of symmetry, the expected asymptotic value for large τ should tend to $\pi/2$ in the case of periodic (or infinite) domains.

We conjecture that the torsion ϑ can be obtained in the limit where the increment size

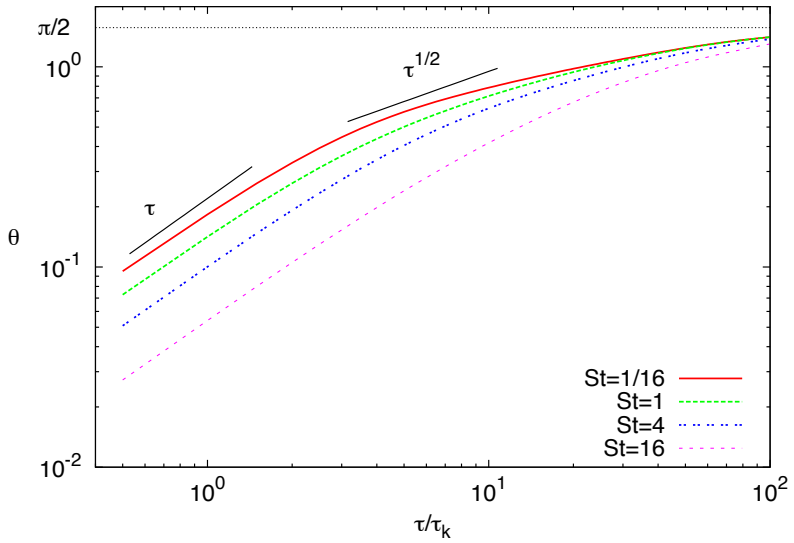

FIGURE 2. Mean curvature angle for homogeneous isotropic turbulence at $Re_\lambda = 100$.

tends to zero,

$$\vartheta(t) \approx \lim_{\tau \to 0} \frac{|\Gamma(t,\tau)|}{2\tau \|\boldsymbol{u}(t)\|} \,. \tag{3.8}$$

The scale-dependent torsion angle can be related to the scale-dependent kinetic helicity (Farge & Schneider 2015), a direction which will be exploited in future work. For inertial particles, we can define the torsion angle analogously by replacing $\boldsymbol{X}$ by $\boldsymbol{X}_p$.

4. Results and interpretation

In the following, we apply the previously introduced multi-scale measures to trajectory data and present the statistical results we obtained.

4.1. *Mean curvature angle*

The mean curvature angle is shown in Figure 2 as a function of τ/τ_k for four Stokes numbers, St $= 1/16, 1, 4$ and 16 in double logarithmic representation. For short time lags, we find a linear scaling behavior in all cases, i.e., we have $\Theta = 2|\boldsymbol{u}_p|\kappa\tau$ for $\tau \to 0$ which is consistent with the mathematical limit in Eq. (3.4). For intermediate values of τ, we do not find the expected inertial range, as observed in Bos *et al.* (2015) for fluid-particles (St=0) at $Re_\lambda = 225$. The explanation is that in the current simulation, the Reynolds number is about a factor two smaller and hence not large enough. For increasing Re, we anticipate a scaling of $\tau^{1/2}$ at least for small Stokes numbers. At long time, we observe that all curves tend towards the expected asymptotic limit of $\pi/2$, which corresponds to decorrelation of the three points. We also see a clear influence of the Stokes number; the curves are shifted to smaller values for increasing St. The inertial particles act as low-pass filters, and we observe for increasing Stokes numbers that the linear behavior is extended so that the expected inertial range for larger Re will disappear for large St.

We also investigated the time development of the mean curvature angle in the context of LES. Trajectories of particles computed in DNS, LES with no particle model (indicated

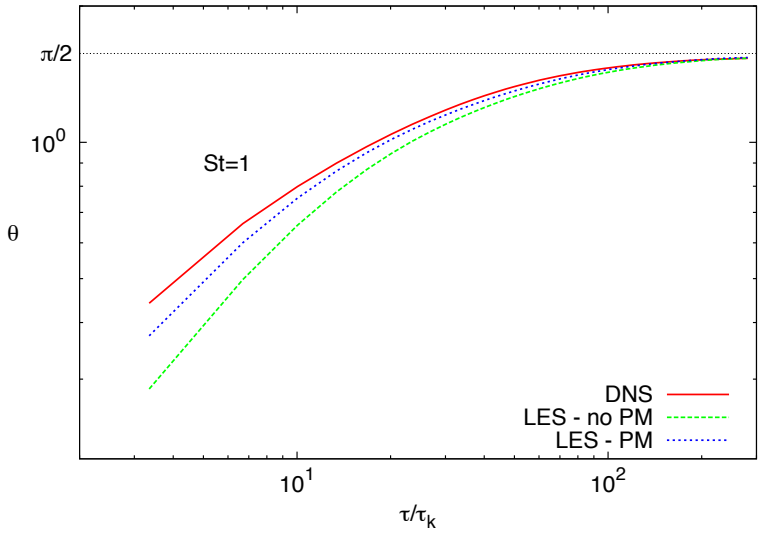

FIGURE 3. Mean curvature angle. DNS - LES comparison. PM = particle model.

by LES – no PM), and LES with particle model (LES – PM) were compared in order to investigate the impact of the unresolved flow scales in LES, as well as the impact of not modeling the unclosed fluctuating velocity along particle trajectories in the particle equation of motion. The model used for the fluctuating velocity is based on the dynamic deconvolution of the LES resolved velocity field using differential filters, which contains no adjustable parameters. For more details about the closure problem arising in one-way coupled simulations of particle-laden turbulent flows, and the model used in the present study, the reader is referred to Park *et al.* (2015) and Park *et al.* (2016). In all LES computations, the subgrid-scale stress tensor is modeled using the dynamic Smagorinsky model (Moin *et al.* 1991).

The computations are performed at a moderate Taylor micro-scale Reynolds number of 85 for particles of unity Stokes number. The DNS grid has 256^3 control volumes, such that $k_{max}\eta = 1.6$. Here, k_{max} corresponds to the cut-off wavenumber and η denotes the Kolmogorow scale. The LES grid is 8 times coarser in each direction. In this regime, the particle trajectories are highly sensitive to the Kolmogorov scales, which are not resolved in the LES.

In Figure 3 we compare the mean curvature angle obtained in DNS, LES – no PM and LES – PM. The LES computation with no particle model yields lower values of the mean curvature angle at short and intermediate times. As already noted, for very short time increments the value of the mean curvature angle is proportional to the curvature of the particle trajectories. Since in LES the smallest resolved eddies are considerably larger than in DNS, and therefore exhibit lower curvature, a decrease in curvature of the particle trajectories is expected in LES in the current regime in which the particles are predominantly slipping on the unresolved small-scale eddies. In conclusion, the mean curvature angle shows improved agreement with the DNS results when the particle model is used.

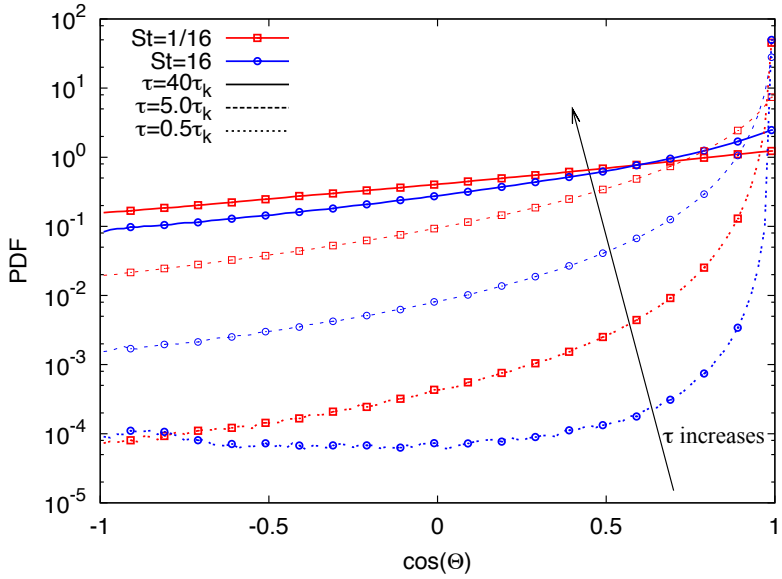

FIGURE 4. PDF of the cosine of the curvature angle for isotropic turbulence at $Re_\lambda = 100$ for $\mathrm{St} = 1/16$ and 16.

4.2. *PDFs of mean curvature angle*

For insight into the higher-order statistics, we show in Figure 4 the probability distribution function (PDF) of the cosine of the curvature angle Θ in log–lin representation for two Stokes numbers, $\mathrm{St} = 1/16$ and 16, considering short, intermediate and long time lags. For increasing time increment size, we observe a transition of the PDF from a Dirac distribution towards a uniform distribution. For short time increments, we find a peak at $\cos\Theta = 1$, which corresponds to a large probability that particles have a directional angle of $\Theta = 0$, i.e., particles are going straight for short time increments. When increasing the Stokes number we observe that the above transition is indeed delayed. Assuming Gaussianity of velocity and acceleration, it was shown in Bos *et al.* (2015) that for $\mathrm{St} = 0$ the PDFs of $1 - \cos(\Theta)$ can be fit with the Fischer $F_{2,3}$ distribution. We anticipate that in the case of finite Stokes numbers the PDFs are again self-similar and can be fit with a corresponding Fischer distribution. Instead of a Gaussian distribution for the signed acceleration components, an alternative approach would be to use a log-normal distribution for the acceleration magnitude. Then we will get a student distribution for the curvature angle PDFs.

4.3. *Mean torsion angle*

The mean torsion angle Γ is shown in Figure 5 as a function of τ/t_k for four Stokes numbers, $\mathrm{St} = 1/16, 1, 4$ and 16 in double logarithmic representation. For large τ values, we again find the asymptotic value of $\pi/2$, which corresponds to decorrelation. We also observe that the slope of the torsion angle is changing with the Stokes number for $\tau \to 0$. Assuming the linear scaling we conjectured (Eq. (3.8)), it is expected that deviation from linear scaling occurs at small time increments for small Stokes, and at larger time increments for larger Stokes (since it increases with the particle characteristic acceleration time scale). We observe this behavior for the mean curvature angle as well. In Figure 5

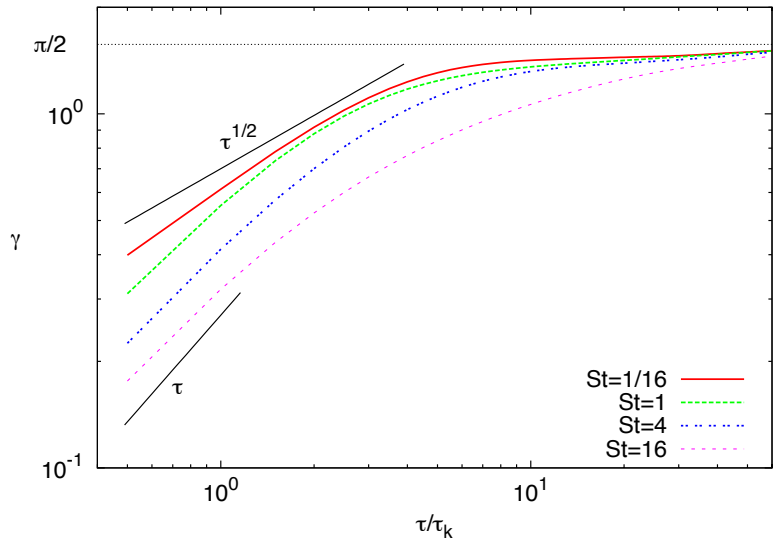

FIGURE 5. Mean torsion angle for homogeneous isotropic turbulence at $Re_\lambda = 100$.

almost linear scaling is observed for the larger Stokes, but not for smaller Stokes, because the time increments are not small enough. For those small Stokes numbers, we observe $\Gamma \propto \tau^{0.6}$. A possible explanation for observing the linear scaling for mean curvature angle but not for mean torsion angle at the same value of the time increment is not yet available, but the observation is probably related to the fact that the definition of the mean torsion angle involves 4 samples, i.e., 3τ, instead of 2τ for the mean curvature angle. We also see that obtaining the asymptotic value is again delayed for increasing St. Extensions of the theoretical predictions are currently under way and will be published elsewhere, as well as the relation to scale-dependent kinetic helicity.

4.4. *PDFs of mean torsion angle*

The probability distribution function of the torsion angle is shown in Figure 6 in log-linear representation for four Stokes numbers, St $= 1/16, 1, 4$ and 16, considering short, intermediate and long time lags. For increasing time lags, we observe flattening of the PDFs in all cases, which corresponds to equidistribution of the angle and again shows decorrelation of the four points. As shown before for the curvature angle, the transition is delayed when the Stokes number increases. For short time lags, we find a higher probability for values of $\Gamma = 0$, which shows that particles have the tendency to remain in the plane of motion.

5. Conclusions and perspectives

We proposed new numerical multi-scale diagnostics for Lagrangian statistics of particle-laden flows. We analyzed trajectories of fluid and inertial particles in isotropic turbulence computed using DNS and LES. First, we extended the multi-scale curvature angle to inertial particles. Thereby, the directional change of particles could be analyzed at different scales using three particle positions of a given trajectory. For the mean angle, we observed linear scaling for small time lags, although an inertial range was absent, probably due

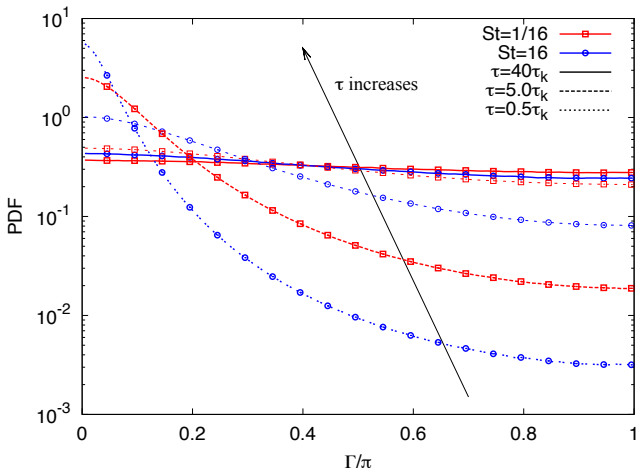

FIGURE 6. PDF of torsion angle for isotropic turbulence at $Re_\lambda = 100$.

to the limited Reynolds number. For large times, we observed an asymptotic limit corresponding to decorrelation of the three positions. The corresponding PDFs gave insight into higher-order statistics.

Then we introduced a novel measure, the multi-scale torsion angle, which quantifies the directional change of particles out of the plane using four particle positions. We analyzed the scaling of the mean torsion angle and the corresponding PDFs for different Stokes numbers. A theoretical justification will be given in future work.

For the above measures, we observed that increasing the Stokes number delays the transition in the statistics from small to large scales. An interesting follow-up from the current work will be to study flows at higher Reynolds numbers, especially with respect to the existence of an inertial range, and of confined flows.

We also assessed the impact of LES and particle SGS modeling. Although the particle SGS model did not recover the missing subgrid scales, we found that it still partially recovers the higher value of the curvature observed in the DNS. The mean curvature angle showed improved agreement with the DNS results when the particle model was used.

The multi-scale tools described in the present study can help investigating the performance of particle SGS models, and in bringing new insights regarding possible improvements. The long-term perspective arising from this work is to develop accurate particle subgrid-scale models which may take into account some of the geometrical information of the trajectory.

In conclusion, the statistical tools yield new insight into the multi-scale statistics of particles in turbulent flows. They are also attractive for experimentalists since only particle positions are required to compute the position increments necessary for the curvature and torsion angle. Possible fields of future applications of the developed tools are in oceanography, for example, trajectories of buoys; in meteorology, for example, the trajectories of balloons; and in electrically conducting fluids (plasmas) for analyzing trajectories of electrons and ions.

Acknowledgments

MF and KS thankfully acknowledge financial support and hospitality from CTR. The authors thank Jeremy Horwitz for fruitful discussions during the Summer Program. For this

work we were granted access to the HPC resources of Aix-Marseille Université financed by the project Equip@Meso (ANR-10-EQPX-29-01). The authors also acknowledge use of computational resources from the Certainty cluster awarded by the National Science Foundation to CTR.

REFERENCES

Bassenne, M., Urzay, J., Park, G. I. & Moin, P. 2016 Constant-energetics physical-space forcing methods for improved convergence to homogeneous-isotropic turbulence with application to particle-laden flows. *Phys. Fluids* **28**, 035114.

Bec, J., Biferale, L., Boffetta, G., Celani, A., Cencini, M., Lanotte, A., Musacchio, S. & Toschi, F. 2006 Acceleration statistics of heavy particles in turbulence. *J. Fluid Mech.* **550**, 349–358.

Bos, W.J.T., Kadoch, B. & Schneider, K. 2015 Angular statistics of Lagrangian trajectories in turbulence. *Phys. Rev. Lett.* **114**, 214502.

Braun, W., De Lillo, F. & Eckhardt, B. 2006 Geometry of particle paths in turbulent flows. *J. Turbul.* **7**, N62.

Burov, S., Tabei, S.M. A., Huynh, T., Murrell, M. P., Philipson, L. H., Rice, S. A., Gardel, M. L., Scherer, N. F. & Dinner, A. R. 2013 Distribution of directional change as a signature of complex dynamics. *PNAS* **110**, 19689.

Constantin, P. Vicol, V. & Wu, J. 2015 Analyticity of Lagrangian trajectories for well posed inviscid incompressible fluid models. *Advan. Math.* **285**, 352–393.

Esmaily-Moghadam, M. & Mani, A. 2015 An analytical description of clustering of inertial particles in turbulent flows. arXiv:1510.00776.

Farge, M. & Schneider, K. 2015 Wavelet transforms and their applications to MHD and plasma turbulence: a review. *J. Plasma Phys.* **81**, 435810602.

Jung, J., Yeo, K. & Lee, C., 2008 Behavior of heavy particles in isotropic turbulence. *Phys. Rev. E* **77**, 016307.

Kadoch, B., Bos, W.J.T. & Schneider, K. 2016 Directional change of fluid particles in two-dimensional turbulence and of football players. *Phys. Rev. Fluids* (submitted).

Moin, P., Squres, K. Cabot, W. & Lee, S. 1991 A dynamic subgrid-scale model for compressible turbulence and scalar transport. *Phys. Fluids A* **3**, 2746–2757.

Park, G. I., Bassenne, M., Urzay, J. & Moin, P. 2015 A dynamic subgrid-scale model based on differential filters for LES of particle-laden turbulent flows. *Annual Research Briefs*, Center for Turbulence Research, Stanford University, pp. 17–26.

Park, G. I., Bassenne, M., Urzay, J. & Moin, P. 2016 A simple dynamic subgrid-scale model for LES of particle-laden turbulence. *Phys. Rev. Fluids* (submitted).

Scagliarini, A. 2011 Geometric properties of particle trajectories in turbulent flows. *J. Turbul.* **12**, N25.

Sposito, G. 2001 Topological groundwater hydrodynamics. *Adv. Water Resour.* **24**, 793–801.

Toschi, F. & Bodenschatz, E. 2009 Lagrangian properties of particles in turbulence. *Annu. Rev. Fluid Mech.* **41**, 375.

Yeung, P.K. 2002 Lagrangian investigation of turbulence. *Annu. Rev. Fluid Mech.* **34**, 115.